LL

EUROPEAN ORGANIZATION FOR NUCLEAR RESEARCH

CERN LIBRARIES, GENEVA

CERN-AT-95-39

CERN AT/95-39 (MA)
LHC Note 354

ge 9742

A Computer Program for the Design of Superconducting Accelerator Magnets

S. Russenschuck

CERN is preparing for the construction of the Large Hadron Collider (LHC), to be installed in the existing LEP tunnel. The LHC requires superconducting magnets which are characterized by the dominance of the coil geometry for the field distribution. The program package ROXIE has been developed for the design and optimization of the coil geometries in two and three dimensions. The paper describes the features of the program, the mathematical optimization techniques applied and gives examples of the recent design work carried out.

Invited Paper presented at ACES'95, March 20-24 ,1995
11th Annual Review of Progress in Applied Computational Electromagnetics,
Monterey, CA, USA

Geneva, Switzerland
26 September 1995

A COMPUTER PROGRAM FOR THE DESIGN OF SUPERCONDUCTING ACCELERATOR MAGNETS

S. Russenschuck,
CERN, 1211 Geneva 23, Switzerland

CERN is preparing for the construction of the Large Hadron Collider (LHC), to be installed in the existing LEP tunnel. The LHC requires superconducting magnets which are characterized by the dominance of the coil geometry for the field distribution. The program package ROXIE has been developed for the design and optimization of the coil geometries in two and three dimensions. The paper describes the features of the program, the mathematical optimization techniques applied and gives examples of the recent design work carried out.

INTRODUCTION

The Large Hadron Collider (LHC) project is a superconducting accelerator for protons, heavy ions and electron- proton collisions in the multi-TeV energy range to be installed at CERN in the existing LEP tunnel with a circumference of about 27 km. The new facility will mainly consist of a ring of high field superconducting magnets cooled to 1.9 K with superfluid helium [21]. The main dipole magnets will operate at about 8.4 T and the quadrupoles at 220 T/m field gradient. The superconducting magnets are characterized by the dominance of the coil geometry for the field distribution. Therefore, the design computations start by optimizing the coil geometry in two and three dimensions, using analytical integration for computing the magnetic field. Contradictory parameters such as maximum dipole field, minimum content of unwanted multipoles and sufficient safety margin for the conductor must be optimized. The keystoning of the conductors and the grading of the current densities between the two layers complicate the task of finding the best solution. The report describes the ROXIE Fortran program (**R**outine for the **O**ptimization of coil **X**-sections, **I**nverse field computation and coil **E**nd design) which has been developed for the coil optimization and which is available for general use on CERNs Risk6000 workstation cluster PaRC.

It is in the coil end regions of superconducting magnets where most of the quenches occur. Therefore special attention is paid to the design of the coil ends with the objectives of a low peak field and a low integrated multipole content. A 3D option in ROXIE allows the geometric position of the cables and the field in the end region to be calculated with a high accuracy. A further area of application for ROXIE is the need to trace back the origins of measured field imperfections. The mechanical dimensions of the active parts of the coils are impossible to verify under their operational conditions, after their deformation due to manufacture, warm pre-stressing, cool-down and excitation. The inverse problem solving consists of using optimization routines to find distorted coil geometries which produce exactly the multipole content measured. For the solving of the optimization problems and the inverse field calculation a number of mathematical programming techniques have been implemented. They will be described in this paper.

FEATURES OF THE ROXIE PROGRAM

The development of the program was driven by three main objectives: To write an easy-to-use program for the design of superconducting coils considering field quality, quench margin and persistent current multipoles, to include the program into a mathematical optimization environment and to develop an integrated design tool with sophisticated graphic routines, interfaces to CAD systems, numerical field calculation codes and a 5 axis milling machine.

The program includes routines to define geometrically coil cross sections and coil ends of dipoles, quadrupoles, sextupoles, octupoles and decapoles made of Rutherford type superconducting cables. The geometric position of coil block arrangements in the cross section of the magnets is calculated from given input data such as the number of conductors per block, conductor type (to be specified in a separate input file), radius of the winding mandrel and the positioning and inclination angle of the blocks, fig. 1. The

fact that the keystoning of the cables is not sufficient to allow their edges to be positioned on the curvature of a circle, is fully respected. This effect increases with the inclination of the coil blocks versus the radial direction. Rectangular shaped coil blocks are also possible if the cable is not keystoned. Cold conditions can be simulated by means of a contraction coefficient. Furthermore the coil can be subjected to elliptic deformation. The input parameters for the coil end generation are the z position of the first conductor of each coil block, its inclination angle, the straight section and the size of the wedges between the conductors, fig. 5. Four options are available: Coil end design with shims between the turns and conductors placed on the winding mandrel, fig. 5, coil end with grouped conductors aligned at the outer radius of the endspacers, fig. 6, coil end for magnets with rectangular cross sections, fig. 13, and racetrack coil ends. It is assumed that the upper edges of the conductors follow ellipses or circles in the developed sz plane defined by their radial position in the straight subsection and the z position in the yz plane, fig. 7. The curvature of the lower edge of the conductor is then calculated assuming constant perimeter. The geometric positions of bare conductors can be printed in different formats suitable for other numerical field calculation packages such as ANSYS and POISSON. In addition the form of the end spacers is constructed and an option allows to print polylines which give the input to a 5 axis milling machine.

The field calculation part allows the calculation of magnetic field, Lorentz - forces, field quality (multipole content) and quench margin. Each conductor is approximated by line currents carrying the same current located at the strand position inside the conductor. The grading of the current due to keystoning of the cable is therefore considered. By applying Biot-Savart's law for each line current, the field is calculated at a given radius in the aperture and the peak field in the coil itself is evaluated. Thus it is possible to calculate the multipole content and the peak field in the coils with a higher accuracy than with finite-element calculations (this is useful, as the multipoles to be minimized create fields of the order of $10^{-7}T$ at the nominal radius). The influence of the iron yoke can be taken into account by imaging the line currents thus assuming that the yoke iron has an infinite permeability. It is foreseen to apply the volume integral method for the consideration of the iron magnetization. For the peak field calculation the influence of the self field of each strand is neglected. As the critical current density has been measured for a strand without compensation for the self field the correct load line characteristic curves are obtained when the self field is neglected in the calculations. An option allows, however, to take the self field into consideration. The self inductance of the coil is investigated by calculating the vector-potential in the coil and the flux linkage is then evaluated by means of Stokes theorem, neglecting the inner inductance of the strands. From the given self inductance the stored energy is calculated. There is an option for the automatic calculation of the mutual inductances between inner and outer layer blocks in both the upper and lower coil. During ramp of the superconducting LHC magnets from 0.58 to 8.4 T nominal dipole field additional currents (persistent currents) are induced in the filaments. These currents which consist of surface currents and currents in the bulk of the superconductor persist for long periods as they decay only through flux creep. The influence of these currents on the field quality can be evaluated. For the 3D field calculation each conductor is sliced up into "bricks" containing line currents the same way as in the 2 dimensional case. The minimum radius of curvature in the bricks is then approximated by means of central differential quotients. The variation of the field on the position of a line current (roller coaster track) can be plotted versus the number of the brick. In addition the integrated multipole content and the field along a line defined by their 3 start and 3 end coordinates can be calculated and plotted. Another feature is the calculation of the cross talk from one coil end to the other, i.e. the integrated multipole content in the end of aperture 2 is investigated which is excited by the current in aperture 1. For the integrated multipole content the iron yoke can be considered by means of image currents whereas for 3D peak field calculations the influence of the iron yoke has to be neglected as in this case the imaging method gives incorrect results. Asymmetric coil ends can also be evaluated; this is necessary for the connection end of the magnets and for the calculation of effects coming from asymmetric coil block displacements in the ends. A particular effect which can be studied is a different length of the upper and lower pole of the dipole magnets.

From the beginning, the program has been structured to allow the application of mathematical optimization techniques. It has been put into an environment of mathematical optimization, with numerous methods available for decision making, treatment of nonlinear constraints and optimization algorithms. All input data can be addressed as design variables of the optimization problem or as an objective (e.g. when

a certain geometrical dimension has to be minimized). All the evaluated field quantities can be addressed as objectives for the optimization. Decision making methods such as objective weighting, distance function, constraint formulation or the automatic set up of payoff tables are implemented. Nonlinear constraints can be treated either by a feasible domain method, the penalty transformation, the augmented Lagrangian function or the boundary search along active constraints. Optimization algorithms such as EXTREM, Rosenbrock, Levenberg-Marquard, Davidon-Fletcher-Powell and genetic algorithms are implemented. In addition there is a sensitivity analysis with Lagrange multiplier estimation available in order to find the hidden resources of a particular design.

Sophisticated graphic routines have been developed for display of geometry, field, forces etc. both in 2D and 3D. The options for 3D contain hidden surface removal, and depth sort algorithm subroutines. The program uses only a few primitives from the GKS library and can therefore easily be modified for other platforms. ROXIE can plot the geometry of the coil in 2 and 3D, the copper wedges between coil blocks and the end spacers for the coil end region. Displacement vectors for coil positions in the distorted case can be plotted, fig. 4, as well as short circuit currents detected by inverse field calculation from time dependant multipoles. Optional is a heading with comments, time and date. The following field quantities can be displayed in the coil cross section: Magnetic field and Lorentz force components in cartesian or local conductor coordinate systems, Vector potential A, current on strand position, current density in the element, in the superconductor and in the copper, and magnetization vector due to persistent currents. In 3D the graphic routines include: Field along a "roller coaster" track in the conductor, 3D magnetic field in the aperture represented by cones, fig. 11, minimum and maximum local field in the coils, Lorentz forces normal to the cable surfaces, fig. 14, Lorentz forces (cartesian vectors) acting on each cable, and minimum radius of curvature of the conductor.

Fields of application are the calculation and optimization of symmetrical magnet structures with superconducting coils made of Rutherford type conductors, calculation of effects coming from asymmetries (geometric errors in the coils due to manufacturing process) both in 2D and 3D and inverse field problem solving for tracing back these effects from field measurements. Further applications are combined function magnets of various kinds, asymmetries in the ramp and splice region, cross-talk between the apertures in the two-in-one type magnets, design and optimization of the coil end region. The features shall be described in more detail with an example from each of the main fields of application.

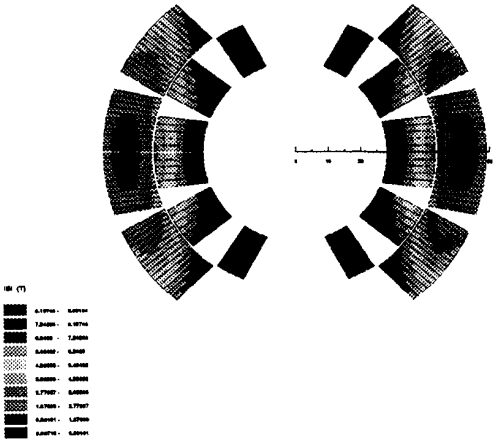

Fig. 1: Optimized dipole coil with 5 block structure (MBPN and MBSMSO models). Display of the magnetic field modulus.

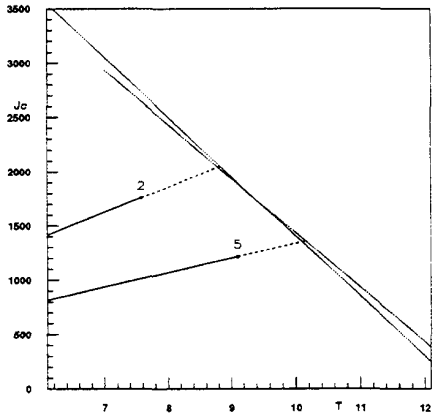

Fig. 2: Load line characteristic curves for the 5 block dipole coil, as displayed in fig.1. Block 2 outer layer, block 5 inner layer.

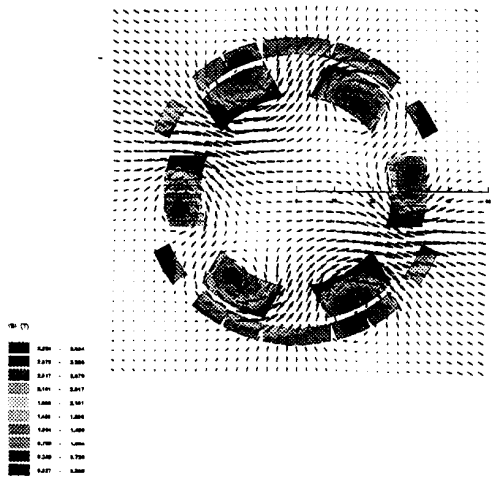

Fig. 3: Cross section of combined dipole-sextupole corrector, with field vector display and $| B |$ in coils

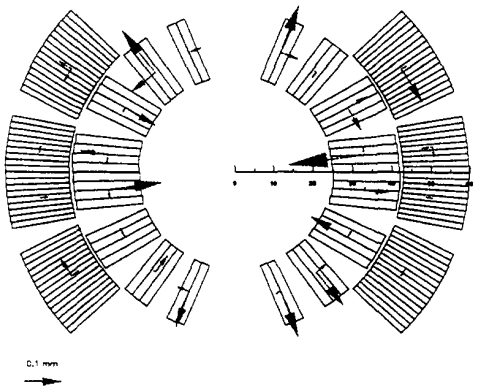

Fig. 4: Displacement vectors for inverse field problem solving for the main dipole model magnet MTA.

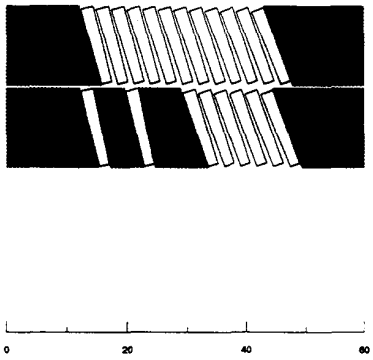

Fig. 5: Cut of main quadrupole end with conductors placed on the winding mandrel.

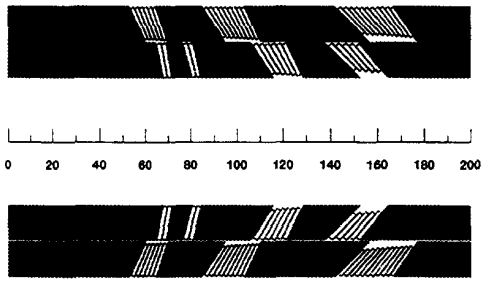

Fig. 6: Cut of model dipole end MBSMSO with grouped conductors aligned on the outer radius.

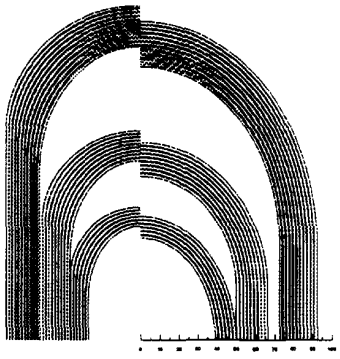

Fig. 7: Developed view on conductors in the dipole end with grouped conductors, outer layer, right: upper edge, left: lower edge.

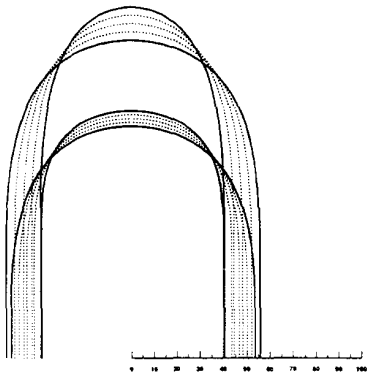

Fig. 8: Polygons for endspacer machining with 5 axis milling machine for dipole model magnet.

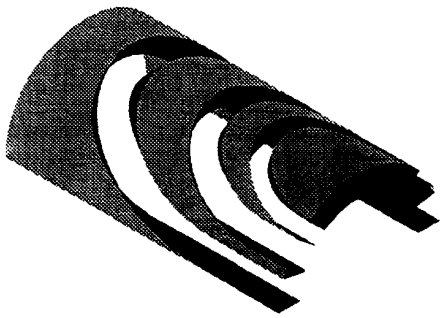

Fig. 9: 3D representation of endspacers for dipole model with grouped conductors (MBSMSO model), outer layer

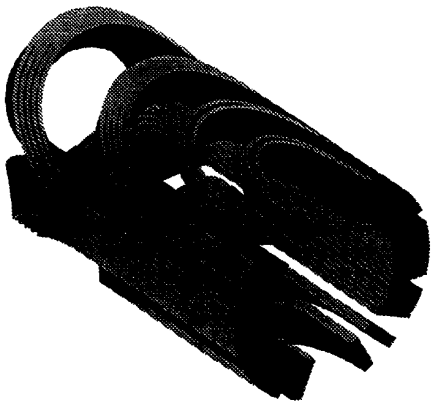

Fig. 10: 3D representation of coil end of the MBFISC dipole model magnet with coordinate system, inner layer only

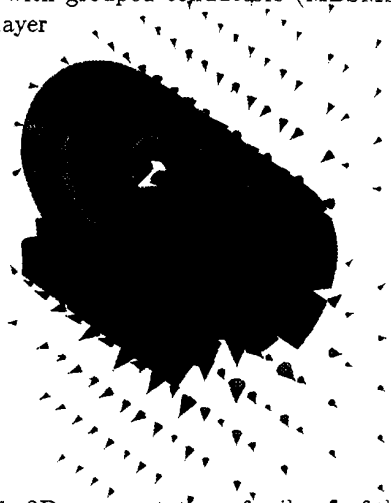

Fig. 11: 3D representation of coil end of the MBTRA dipole model magnet with magnetic field cones.

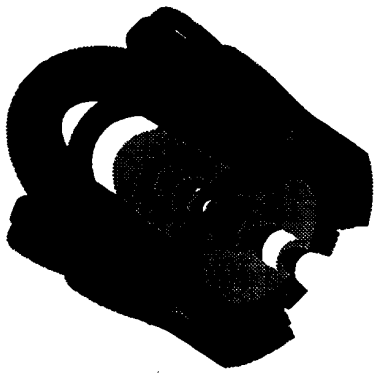

Fig. 12: 3D representation of coil end of the insertion quadrupole

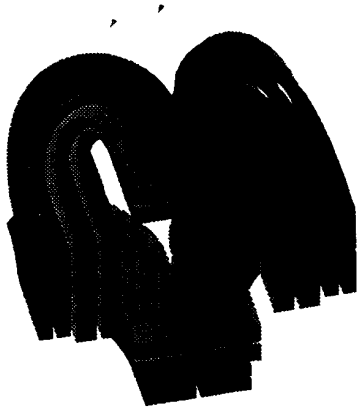

Fig. 13: 3D representation of coil end for a insertion quadrupole design with rectangular coil cross section.

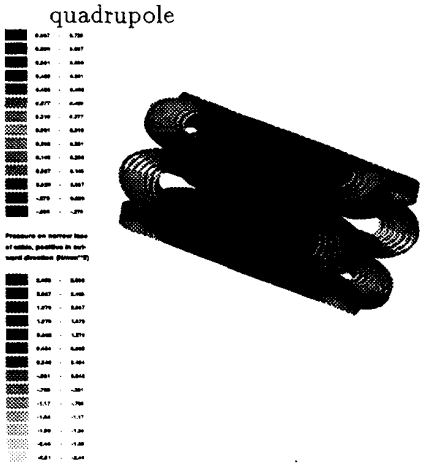

Fig. 14: 3D view of sextupole corrector coil, with pressures due to Lorentz-forces on cables.

MATHEMATICAL OPTIMIZATION TECHNIQUES

Mathematical optimization including numerical techniques such as linear and nonlinear programming, integer programming, network flow theory, and dynamic optimization has its origin in operations research developed in response to military needs of world war II. An optimality criterion for optimization problems with conflicting objectives has been introduced by Pareto in 1896 [20]. The solution process for vector-optimization problems is threefold, based on decision making methods, methods to treat nonlinear constraints and optimization algorithms to minimize the objective function (we shall call this an optimization procedure). Methods for decision making have been introduced and applied on a wide range of problems in economics by e.g. Marglin 1966 [16] and Fandel 1972 [3]. The theory of nonlinear programming with constraints is based on the optimality criterion by Kuhn and Tucker, 1951 [14] which provided the basis for later developments in mathematical programming. Numerous optimization algorithms both using deterministic and stochastic elements have been developed in the sixties. Researchers tend to come back to genetic and evolutionary algorithms recently as they are suited for parallel processing, Fogel 1994 [6], Holland 1992 [10]. While desktop computing power to date is available which was ten years ago only accessible in large computer centers, the combination of mathematical optimization techniques and field calculation has become a modern tool for electrical engineering.

Characteristic for real-world optimization problems are multiple conflicting objectives which should be considered simultaneously Usually the individual solutions for each single objective function differ and a solution that maximizes one objective will not, in general, maximize any of the other objectives. Any improvement of one objective can be achieved only at the expense of another. For the definition of the optimal solution of these so called vector-optimization problems we apply the optimality criterion by Pareto 1896 originally introduced for problems in economics. A **Pareto-optimal** solution (for vector maximum problems also called noninferior solution) is given, if there exists no other solution that will yield an improvement in one objective without degradation in at least one other objective. It is clear that this yields a set of solutions rather than one unique solution. The decision maker (who is not always the design engineer undertaking the optimization) usually picks a solution out of a solution set intuitively. Applying mathematical optimization routines, however, requires a formalized decision making method. Below some methods of decision making are briefly described. It can be proved that they possess a substitute problem to the vector optimization problem with a Pareto-optimal solution (assuming convexity of the objective functions). A comprehensive overview on decision making can be found in Cohon, 1978 [2].

The **objective weighting function** is the sum of the weighted objectives $f_k(\vec{X})$ and results in the minimization problem: $min\{u(\vec{F}(\vec{X})) = \sum_{k=1}^{K} t_k \cdot f_k(\vec{X})\}$ with the weighting factors t_k representing the users preference. The design variables are comprised in the vector $\vec{X}$. The problem is to find the appropriate weighting factors in particular when the objectives have different numerical values and sensitivity. Using objective weighting results therefore in an iterative solution process where a number of optimizations have to be performed with updated weighting factors, a cumbersome process if the decision maker is not the analyst undertaking the calculations. The problem of choosing the weighting factors appropriately also occurs when the **distance function method** is applied. Most common is a least squares objective function. With f_k^* being the requirements for the optimum design, the minimization problem reads: $min \parallel \vec{z}(\vec{X}) \parallel_2^2 = min \sum_{k=1}^{K} t_k(f_k^*(\vec{X}) - f_k(\vec{X}))^2$. The disadvantage of least squares objective functions with the euclidean norm $\parallel . \parallel_2$ is the low sensitivity for residuals smaller than one. Therefore sufficiently high weighting factors t_k have to be introduced. If the absolute value norm is applied the disadvantage is the nondifferentiable objective function in the optimum which makes the application of Newton-methods impossible. The problem with the weighting factors can be overcome by defining the problem in the **constraint formulation**. Only one of the objectives is minimized and the others are considered by constraints. The constraints represent the minimum request values specified by the user for the particular objective. The problem is that for badly chosen constraints there exists no feasible solution at all, whereas non active constraints represents a zero weight for the particular objective. However, starting with a design where some engineering expertise was already put into, the analyst should be able to define appropriate constraints. The constraint formulation has the advantage that a **sensitivity analysis** by means of a Lagrange multiplier estimation can be performed using the necessary optimality conditions for constraint optimization problems

introduced by Kuhn and Tucker. The interesting characteristic of the Lagrange multipliers of the corresponding Lagrange function to the constraint problem is that they are a measure of the price which has to be paid when the constraint is decreased. The decision maker can then explore the hidden resources of a design. A tool which provides the decision maker with a lot of information about the hidden resources of a design is the **payoff table**. To create this table K individual constraint optimization problems are solved to find the best solution for each of the K objectives. Best compromise solutions can then be found by minimizing the "distance" from the in general nonfeasible "perfect solution" applying different norms e.g. L_1, L_2 and L_∞ .

Decision making is the most important part and influences the convergence behavior of the whole optimization procedure. For the minimization of constrained and unconstrained objective functions numerous methods have been proposed in the last 30 years. It is most important to find the right minimization method to fit with the method of decision making.

As the design variables of the optimization problem can usually only be varied between upper and lower bounds, a modified objective function is applied $p(\vec{X}) = f(\vec{X})$ if no bound is violated and $p(\vec{X}) = f(\vec{X}^*) + r(\vec{X})$ if a bound is violated. $\vec{X}^* = (x_1, x_2, ..., x_l^*, ...x_n)$ and $r(\vec{X}) = (x_l - x_{lu})^2$ $x_l^* = x_{lu}$ if $x_l > x_{lu}$, $r(\vec{X}) = (x_{ll} - x_l)^2$ $x_l^* = x_{ll}$ if $x_l < x_{ll}$. r_l is a sufficiently high penalty parameter. The advantage of this procedure is that the violation of the bounds are checked before a function evaluation is carried out and that the existing algorithms for unconstrained minimization can be applied without modifications. The objective weighting function as well as the distance function method allows the immediate application of an algorithm for finding the minimum value of an unconstrained objective function as there are no nonlinear constraints to be considered. With the constraint formulation the problem of the treatment of the nonlinear constraints arises. One method is the transformation of the constrained problem into a unconstrained problem by means of a **penalty function** method. The main idea is to add a penalty term to the objective function which depends on the degree to which the constraints are violated and vanishes if the constraints are satisfied. The constraint optimization problem $min\, f(\vec{X})$ subject to equality constraints $h_j(\vec{X}) = 0$ and inequality constraints $g_i(\vec{X}) \leq 0$ transformed into the penalty function to be minimized reads:

$$p(\vec{X}) = f(\vec{X}) + \sum_i p_i \cdot max^2(0., g_i(\vec{X}) - c_i) + \sum_j p_j (h_j(\vec{X}) - d_j)^2 \qquad (1)$$

In order to achieve feasibility of the result the penalty factors p_i, p_j have to be chosen relatively large. Large penalty factors, however, lead to ill-conditioned function topologies, and the optimization algorithms need many function evaluations to find the minimum. It was therefore proposed to solve a sequence of unconstrained minimization problems with increasing penalty factors, **SUMT** or to add the penalty terms to the corresponding Lagrange function, **method of augmented Lagrangian**. Replacing the squares in (1) by the absolute value leads to the **exact penalty transformation** where the penalty factors can be reduced. The problem here is the nondifferentiability of the objective function for active constaints. If the number of design variables does not exceed 5, the method of **boundary search along active constraints** can efficiently be used. The ROXIE user has the choice between the above mentioned methods. It needs some experience to select an efficient procedure consisting of decision making, treatment of nonlinear constraints and a suitable optimization algorithm.

The following optimization algorithms are available: Optimization algorithm **EXTREM by Jacob** [11] which consists of one-dimensional minimizations by means of Powell extrapolations [22] in a main search direction (user supplied) and a orthogonal direction evaluated by Gram-Schmidt orthogonalization. After these one-dimensional searches have been carried out (end of the i-th step) the main search direction is updated by a vector pointing from the initial outline to the minimum of the i-th step. The user has to supply an initial step-size which is taken to $(x_{lu} - x_{ll})/10.$. This user-friendly algorithm is suitable for practically all applications. The **parametric study** evaluates the objective functions for all the combinations of different design variables where for each design variable 10 different values are taken. As the total number of function evaluations is therefore 10^n (for n design variables) the parametric study is only appropriate for up to 3 design variables. The **sensitivity analysis** calculates the sensitivity due to errors in the design variables. A Jacobian Matrix is printed out. It consists therefore of n+1 function evaluations. The **Levenberg-**

Marquard algorithm [13] was originally developed for nonlinear regression problems using least squares objective functions. We can apply it therefore efficiently to the distance function problem. To check the necessary optimality conditions for constraint problems (Kuhn-Tucker equations) a **Lagrange-Multiplier estimation** can be carried out minimizing the corresponding Lagrange- function. The Lagrange function is minimized using the **Davidon-Fletcher-Powell** algorithm where the step-size and direction is given by $\Delta\vec{X} = -H^{-1}\nabla f(\vec{X})$ The Hessian Matrix H does not have to be calculated in each point but is updated iteratively beginning with the unity Matrix I. As the "design variables" are the Langrange - multipliers $\vec{\alpha}, \vec{\beta}$ to be estimated, the derivatives in α_i, β_ican be approximated with a high accuracy. That is the reason for the good convergence behavior of this method when applied to the Lagrange multiplier estimation. It can, however, be applied also to all the other design optimization problems, the convergence behavior is then dependent upon the function topology. In **genetic algorithms**, each trial solution is coded as a vector (chromosome) $\vec{X}$ with elements being described as genes. Holland [10] suggested that the chromosomes are represented by binary strings. It is obvious that this algorithm is specially suited for integer programming. From two sets of chromosomes offspring are produced by use of genetic operators such as crossover and mutation. Crossover means the interchanging of sections of the chromosomes between two parent chromosomes. The position where the chromosomes are split into two sections is chosen randomly. Mutation means that with a certain likelihood single bits in the chromosomes are flipped. As an example, let be the parent chromosomes 000100110|1010111 and 110001010|1100011 , then the offspring is created by crossover (| indicates the crossover point) 000100110|1100011, 110001010|1010111. In order to avoid the dominance of "superindividuals" which leads to an uniform population unable of further evolution, a sufficiently large gene pool has to be chosen from which offspring are created by mating pairs of chromosomes. The likelihood of reproduction for each chromosome is then proportional to the objective function value for the particular design represented by the chromosome. From the offspring the fittest strings are used for the next generation. Only about 60% of the population is used for crossover (crossover probability 0.6). The others simply survive and ensure the genetic diversity of the population. The bit mutation probability is 0.001 which means that only every 1000 th bit is mutated. The problem of genetic algorithms is the dependance of the solution on user supplied and problem dependent input such as crossover probability, size of the gene pool etc. More research has to go into making the algorithm more robust for every day use in optimization of superconducting magnets.

EXAMPLES

Dipole coil optimization (cross section)

Because of the length of the dipole magnets (about 13 m) the design optimization starts with the 2D cross-section of the coils. The design variables for this optimization problem are the positioning angles and the inclination angles of the coil blocks (8 or 10 design variables depending on the number of blocks chosen), c.f. fig. 1.

The field quality of a magnet is usually described by the B_n (called the normal) and the A_n (called the skew components) of the field defined by the expansion of the complex field: $B_y + iB_x = \sum_{n=1}^{\infty}(B_n + iA_n)z^{n-1}$ with $z = x + iy = re^{i\varphi} = r(\cos\varphi + i\sin\varphi)$ and $B_\varphi + iB_r = (B_y + iB_x)e^{i\varphi}$. In ROXIE the r- component of the field is calculated directly by means of the Biot-Savarts law. $B_r(\varphi)$ at a given radius $r = r_0$ is then harmonically analyzed by means of the program TRICOF from the CERN Library which has been set up for double precision for higher accuracy. With A being usually defined as the coefficients of the cos terms and B being the coefficients of the sin terms we get from given equidistant function values in the interval $-\pi \leq \varphi \leq \pi$: $B_r(r_0) = \sum_{n=1}^{\infty}(B_{n(r_0)}\sin n\varphi + A_{n(r_0)}\cos n\varphi) = B_0(r_0)\sum_{n=1}^{\infty}(b_n \sin n\varphi + a_n \cos n\varphi)$. The A and B terms are in agreement with the above definition for the unit radius. The optimization problem possesses a number of different objectives which are partially contradictory:

- A main dipole field of 8.65 T
- A small sextupole field comp. (b_3 = min) and a small decapole field comp. (b_5 = min)
- $b_7 < 0.02 \cdot 10^{-4}$ and $b_9 < 0.005 \cdot 10^{-4}$
- Minimum volume of superconductor
- Maximum margin to quench
- Small multipole content due to persistent currents

By applying the objective weighting function with recursively updated weighting factors and the algorithm EXTREM, a design with only five coil blocks could be found which perfectly meets the requirements concerning field quality as given from beam simulations. All previous design studies considered a six block design. Numerical results are given in Table 2 (MBPN and MBSMSO models), the cross section is displayed in fig. 1. The deterministic optimization procedure converges very well and minimizes the weighting function usually in about 200 function evaluations. However, for each run the number of blocks and the number of conductors per block has to be selected and kept constant. This way, the optimization routine cannot be used to discover a new design principle.

An approach for a "creative" design tool could be the use of genetic algorithms. As they are specially suited for integer programming a optimization problem was set up with predefined conductors (48 in the outer layer, 26 in the inner layer) where by means of genetic algorithms the current was switched on and off, thus resulting in bit strings (genes) of size 74. The size of the gene pool was 65, the crossover probability 0.6 and the bit mutation rate 0.001. As in this case the number of conductors is not fixed, a minimum number of turns was included as an additional objective in the weighting function. Fig. 15 shows some intermediate steps of the minimization after 65, 195 and 4550 function evaluations. The new idea which could be derived is that by piling up some more conductors in the outer layer results in a shielding effect and the pole angle of the inner layer can be increased. A design derived from this idea using the same cable as for the 5 block design (fig. 1) can be seen in fig. 15 on the right. Both designs, although quite different, use the same amount of superconductor, have both the same high field quality and the same margin to quench in the inner layer. Advantageous of the design in fig. 15 is the larger pole angle in the inner layer, which results in easier to wind coil ends. Disadvantages are the higher current density in the cable necessary to produce the same main field (resulting in higher hot spot temperatures at quench) and the reduced margin to quench in the outer layer.

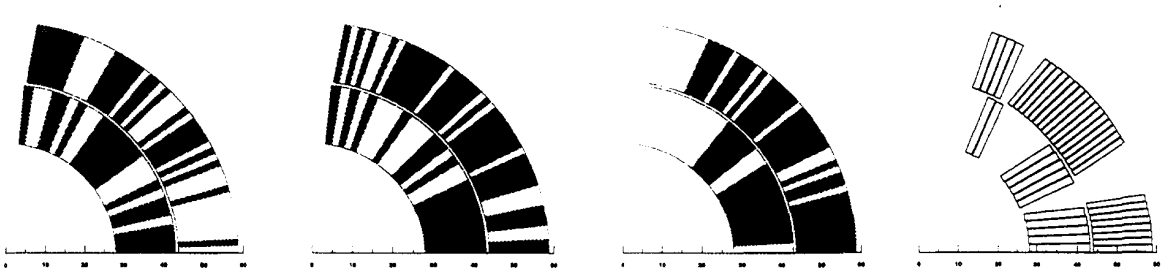

Fig. 15: Intermediate steps of the optimization using genetic algorithms after 65, 195 and solution after 4550 function evaluations (from left to right). A feasible design derived from the solution by means of deterministic methods using the same cable as the 5 block design (fig.1) is displayed on the right.

The main quadrupole as an inverse field problem

With a slightly modified input file ROXIE is able to calculate multipole errors, peak field etc. in asymmetric coil block arrangements. This is the basis of the inverse field calculation option for the tracing back of conductor displacements from given field harmonic measurements. These displacements can well be asymmetric thus requiring individual treatment of each coil block.

The main parameters of the lattice quadrupoles for LHC are a nominal gradient of 252 T/m, a magnetic length of 3.05 m, a nominal current of 15060 A, an inner coil aperture of 50 mm and an operational

temperature of 1.8 K. Before being assembled into their common yoke the two coil-collar assemblies of the second magnet have undergone magnetic measurements at room temperature. Table 1 gives the measured multipole distribution in the straight part of one of these assemblies together with the expected (intrinsic) values.

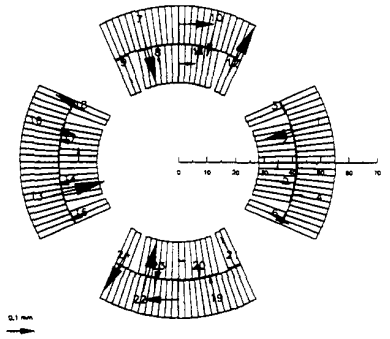

Fig. 16: Displacement vectors for the quadrupole

	Measured		Intrinsic	
n	Normal	Skew	Normal	Skew
1	-	-	-	-
2	-21910.	-	-21910.	-
3	1.972	-5.456	-	-
4	-0.723	-0.920	-	-
5	-0.219	-0.436	-	-
6	-0.066	0.153	-0.79	-
7	-0.004	-0.285	-	-
8	-0.002	0.109	-	-
9	-0.043	-0.022	-	-
10	0.59	-0.044	0.52	-

Table 1: Measured and intrinsic multipole content of the warm quadrupole coils.

The function to be minimized in the inverse field computation problem is a least squares objective function $min\ z(\vec{X}) = min \sum_{i=1}^{10} p_i \cdot ((f_i(\vec{X}))^2 + (g_i(\vec{X}))^2)$ with the residuals $f_i(\vec{X}) = b_i^*(\vec{X}) - b_i$ and $g_i(\vec{X}) = a_i^*(\vec{X}) - a_i$ where $b_i^*(\vec{X})$,$a_i^*(\vec{X})$ are the calculated and b_i,a_i are the measured multipoles. $\vec{X}$ is the vector of the design variables for the inverse problem. The p_i are weighing factors in order to compensate for the different numerical values of the residuals. The design variables are the possible perturbations of the coil blocks, which determine the content of the multipole components. Because of the non-symmetric nature of the geometrical coil positioning errors a high number of design variables results for the inverse field problem. It had therefore to be assumed that the positioning errors hold for an entire coil block rather than individual conductors. Constraints on the block displacements were introduced: At the poles the collar inserts represent a limitation to any azimuthal motion. The blocks adjacent to the horizontal or vertical planes move together azimuthally; this motion may be different for the two layers. In this way a difference of elastic moduli in the coil layers is accounted for. Each block is allowed to move in the radial direction resulting in a total number of 32 design variables for the inverse field problem. It was solved by means of the Levenberg-Marquard algorithm with about 800 function evaluations. The result is displayed in fig. 16. The displacements show no significant inside movement of inner layer blocks. The adopted collaring procedure, where the coil assembly mandrel is extracted before the final compression of the collars, seems therefore acceptable.

Coil end optimization

The design variables for the optimization are the length of the straight section of each block, the ellipticity of the innermost turn of each block and the inclination angle of each of the blocks in the yz plane, c.f. fig. 6. The positioning angle and inclination angle for defining the cross section (xy plane) (fig. 1) of the magnet was kept constant as found by the 2D cross section optimization. The objectives for the coil end optimization are:

- Minimum integrated multipole content in the coil end
- Low enhancement of the field in the coil
- Minimization of the variation of pressure on the narrow face of the conductor due to Lorentz forces in order to avoid slip between turns
- Maximization of the minimum radius of curvature in each coil block
- Short physical length of the end

A short end length and homogenous Lorentz force distribution in the innermost turn, which can be achieved by placing the inner block of the outer layer closer to the straight section of the magnet, leads to a higher peak field to main field ratio. The problem was solved with objective weighting functions and

successively updated weighting factors and the algorithm EXTREM. Table 2 shows the results of the field calculations for different versions of model dipole magnets. 2D cross section optimizations have been carried out for the models MBFISC, MBTRA and MBPN, but only the MBPN and the MBSMSO coil end (which have the same cross section) has been optimized using the described methods. For the optimization of the integrated multipole content the iron yoke is assumed to end at the onset of the coil end (z=0), in order to reduce the peak field in the coil end region. The peak field is related to the dipole field which would occur for the bare coil.

Design	MTA	MBFISC	MBTRA	MBPN	MBSMSO
Aperture Diameter (mm)	50.	56.	56.	56.	
Cable height, inner layer (mm)	17.	16.7	12.3	15.	
Cable height, outer layer (mm)	17.	16.7	11.7	15.	
Number of turns	74	82	98	82	
Beam distance (mm)	180.	200.	180.	180.	
Yoke radius (mm)	93.	91.5	82.	98	
Length of coil end (mm)	215.	163.	140.	191.	178.
Cable length, Inner layer (mm)	3533	4473	8091	5985.	4591.
Cable length, Outer layer (mm)	10229	11658	12830	12752.	11943.
Nominal current (A)	13987.	12844.	8718.	11614.	
Field at nominal current (T)	9.85	9.46	8.65	8.65	
Quench field (T)	10.37	9.96	9.43	9.65	
Self inductance (mH/m)	6.42	7.82	11.41	7.64	
NI/B	105063.	111352.	98773.	110097.	
$b_3(10^{-4}$ at r=10 mm)	0.690	0.046	0.15	-0.345	
$b_5(10^{-4}$ at r=10 mm)	0.110	0.0015	0.0300	0.0244	
$b_7(10^{-4}$ at r=10 mm)	0.150	-0.0088	0.0173	0.0060	
$b_9/(10^{-4}$ at r=10 mm)	0.020	0.0022	-0.0005	0.0000	
$n_3(10^{-4}$ at r=10 mm)	-4.72	-3.09	-3.62	-3.62	
$n_5(10^{-4}$ at r=10 mm)	0.332	0.111	0.121	0.150	
$n_7(10^{-4}$ at r=10 mm)	-0.019	-0.019	-0.027	-0.027	
$n_9/(10^{-4}$ at r=10 mm)	0.009	0.004	0.005	0.006	
Peak field/main field, inner layer, 2D	1.0235	1.0327	1.057	1.051	
Peak field/main field, outer layer, 2D	0.856	0.908	0.892	0.875	
Peak field/main field, inner layer, 3D	1.0473	1.0668	1.107	1.100	1.18
Peak field/main field, outer layer, 3D	0.921	0.992	0.974	0.923	0.709
$\Delta P\ (N/mm^2)$	15.3	10.6	19.2	18.6	15.9
F_z, inner layer (N)	14460.	10171.	16827.	13279.	13940.
F_z, outer layer (N)	29406.	36897.	25645.	31641.	31419.
Ellipticity ratio, Inner layer	0.998	0.963	0.586	0.864	0.714
Ellipticity ratio, Outer layer	1.027	0.939	0.638	0.636	0.762
Min. radius of curvature, inner layer	4.62	14.36	13.89	6.24	14.32
Min. radius of curvature, outer layer	31.1	15.78	34.54	37.24	30.32
$b_3^{**}(10^{-4}$ at r=10 mm)	52.47	22.55	-33.07	0.000	2.05
$b_5^{**}(10^{-4}$ at r=10 mm)	-0.22	0.189	-1.68	0.000	-0.0065
$b_7^{**}(10^{-4}$ at r=10 mm)	0.135	-0.0036	-0.077	0.0049	-0.0442
$b_9^{**}(10^{-4}$ at r=10 mm)	0.0215	0.0069	-0.0031	0.0048	-0.0071

Table 2: Results for the 2D and 3D coil optimizations. b_n normal relative multipoles (2D), n_n normal relative multipoles due to persistent currents at injection energy. Integration path for relative integrated multipole errors b_n^{**} from z=-100mm to z=250 mm. Iron yoke ends at z=0. Ellipticity ratio given for the upper edge of the innermost turn in each layer, ΔP = Variation of pressure due to Lorentz forces on the narrow face of the innermost conductor of the inner layer. ΔP and F_z are given for a current that would give 8.65 T with a iron yoke of 85 mm.

The multipole content given for the cross section shows that the MBFISC,MBTRA and MBPN dipole models have been already successfully optimized in two dimensions. The MBPN and MBSMSO dipole models show significantly reduced integrated multipole content in the ends. The peak field to main field ratio is difficult to reduce since for the cross section optimization more turns are added in the second block of the outer layer. This is done in order to reduce the b_7 and b_9 components, but considerably increases the

peak field in the coil ends which cannot be compensated with the end design. This effect is particularly pronounced in the MBTRA model which uses the small cable of only about 12 mm height and the 5 block design in the cross section. The reduction of the variation of Lorentz forces acting on the narrow face of the conductor which constitutes a source of slip between the conductors is very difficult. It can be done by shifting the inner block of the outer layer towards the center of the magnet as it is done for the MBFISC and the MBSMSO design. The objective conflicts with the required minimum field enhancement in the ends. Therefore a dipole model will be built with a reinforced mechanical construction, the so called end clamping cage.

ACKNOWLEDGEMENT

I thank T. Tortschanoff and N. Siegel for the discussions and ideas which have been incorporated into the program, which at the current 3.4 version led to more than 14000 lines of computer code. Many thanks to R. Wolf who contributed the subroutines for the calculation of the persistent current effects. I would like to express my gratitude to S. Masso who installed the program on CERN's parallel RISC6000 workstation cluster PaRC, as well as to all colleagues and users of ROXIE who helped me testing the versions or provided me with their designs which I could use as examples.

References

[1] Bertsekas, D.P.: Constrained optimization and Lagrange multiplier methods, Academic Press, 1982
[2] Cohon, J.L.: Multiobjective Programming and Planning, Academic Press, New York, 1978
[3] Fandel, G.: Optimale Entscheidung bei mehrfacher Zielsetzung, Springer, Berlin 1972
[4] Fiacco, A.V., McCormick, G.P.: Sequential unconstrained minimization techniques, Wiley, 1968
[5] Fletcher, R., Powell, M.J.D.: A rapidly convergent descent method for minimization, Computer Journal, Vol. 6, 1963
[6] Fogel D.B.: An Introduction to Simulated Evolutionary Optimization, IEEE-Transactions on Neural Networks, 1994.
[7] Fletcher, R., Reeves, C.M.: Function minimization by conjugate gradients, Computer Journal, Vol. 7, 1964
[8] Gill, P.E., Murray, W., Wright, M.H.: Practical optimization, Academic Press, 1981
[9] Himmelblau, D.M.: Applied nonlinear Programming, McGraw-Hill, 1972
[10] Holland, J.H.: Genetic algorithms, Scientific American, 1992
[11] Jacob, H.G.: Rechnergestützte Optimierung statischer und dynamischer Systeme, Springer, 1982.
[12] Krebs, M.: Vergleich unterschiedlicher Methoden zur Behandlung nichtlinearer Restriktionen in Optimierungsproblemen, Diplomarbeit am Institut fuer Elektrische Energiewandlung, Technische Hochschule Darmstadt, Germany, 1990.
[13] Kuester, J., Mize, J.H.: Optimization techniques with Fortran, Mc Graw-Hill, 1973
[14] Kuhn, H.W., Tucker, A.W.: Nonlinear Programming, Proceedings of the 2nd Berkeley Symposium on Mathematical Statistics and Probability, University of California, Berkeley, 1951
[15] Luenberger, D.G.: Introduction to linear and nonlinear programming, Addison-Wesley, 1973
[16] Marglin, S.A.: Objectives of Water-Resource Development in Maass, A. et al. Design of Water-Resource Systems, Cambridge, 1966
[17] Marquard, D.M.: An algorithm for least squares estimation of nonlinear parameters, Society for Industrial and Applied Mathematics, 1963
[18] Morse P.M., Kimball G.E.: Methods of operations research, Wiley & Sons, New York, 1950.
[19] Nelder, J.A., Mead, R.: A simplex method for function minimization, Computer Journal, Vol. 7, 1964
[20] Pareto, V.: Cours d'Economie Politique, Pouge 1896 or translation by Schwier, A.S.: Manual of Political Economy, The Macmillan Press, 1971
[21] Perin, R.: The Superconducting Magnet System for the LHC, IEEE-Transactions on Magnetics, 1991
[22] Powell, M.J.D.: An efficient method for finding the minimum of a function of several variables without calculating derivatives, Computer Journal, 1964